1997 HST Calibration Workshop
Space Telescope Science Institute, 1997
S. Casertano, et al., eds.

HST Observations of the Gravitational Lens Systems HE 1104−1805 and J03.13

M. Remy, J.-F. Claeskens,[1] and J. Surdej[2]

Institut d'Astrophysique, Université de Liège, Belgium

Abstract. High angular resolution PC1 images of the gravitational lens systems HE 1104−1805 and J03.13 are presented. Using a method described in Remy et al. (1997a), optimal TinyTim PSFs are constructed to fit at best the lensed point-like components. The derived photometry of the GL components and the detection of the lens galaxy for HE 1104-1805 are discussed. *Textbook case* FOS spectra of J03.13 A and B clearly show that this double QSO is a cosmic mirage.

1. Introduction

The quasar HE 1104−1805 was discovered to be a gravitational mirage candidate with a redshift $z = 2.303$ by Wisotzki et al. (1993, 1995). Prominent absorption lines in the spectrum of this quasar indicate the possible presence of galaxies at redshifts $z = 1.6616$ (damped Lyα, FeII, MgII) and $z = 1.320$ (MgII) along the line-of-sight (Smette et al. 1995). From the observed spectral variability, these authors report the signature of both intrinsic variations and changes due to microlensing. They stress the importance of direct observations of the lensing galaxy in order to model the macro-lensing configuration in detail.

On the basis of observations obtained with the NOT in February and March 1994, Grundahl et al. (1995) were the first to report the presence of a very red object between A and B at a distance of $1\farcs15$ from A with $I_c \sim 20.6$, the probable lensing galaxy. This detection was subsequently confirmed on the basis of one single ESO NTT 3.5 m frame also obtained in February 1994. A full description of these ground-based NTT and NOT observations is given by Remy et al. (1997b).

Following this first set of observations, we have included HE 1104−1805 as a priority target in the framework of a study of gravitational lensing with HST. The corresponding direct imaging, data reduction, analysis and interpretation are briefly described.

In a search for gravitational lensing within a sample of highly luminous quasars (hereafter HLQs, Surdej et al. 1993), Claeskens et al. (1996) have reported the identification of a new candidate for the quasar J03.13.

Multiple direct CCD frames of J03.13 were taken in November 1995 through the F555W and F814W filters with the WFPC2 camera onboard HST. In addition, good S/N, low-resolution FOS spectra of J03.13 A and B were obtained in October 1996. A summary of all these data and their interpretation is also presented.

2. PC1 Direct Imaging of HE 1104−1805

One HST orbit was allocated to the planetary camera (PC1) observations of HE 1104−1805, which took place on November 23, 1995. Based on the photometry already reported for this

[1]Research Assistant (FNRS, Belgium)

[2]Research Director (FNRS, Belgium)

system from ground-based observations, our strategy was to obtain 2 exposures of 100 s with the F555W filter (nearly Johnson V), 4 exposures of 200 s with F814W (nearly Kron-Cousins I_c) and 2 additional 100 s exposures with F814W. We chose the ADC channel with 14 e^-/ADU gain. Offsets by $\simeq 1\farcs6$ were introduced between the exposures in order to optimally dither the QSO images and to more easily detect faint structures at small angular scales.

Composite F555W and F814W images of the quasar, made after proper re-centering and coaddition of the single PC1 frames, are shown in the upper panels of Figure 1. We immediately notice on the composite F814W image a diffuse object between A and B, identified as the lensing galaxy G. This object is not detected in the composite F555W image. The projected position of its peak is distant from A by about one third the angular separation ($3\farcs193$) between A and B. Note that the galaxy is not exactly co-aligned with A and B.

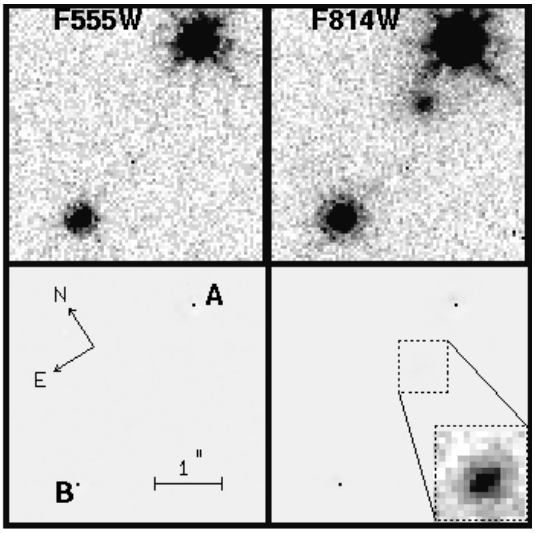

Figure 1. Composite F555W (upper left panel) and F814W (upper right panel) PC1 CCD frames of HE 1104−1805. From the F555W data, we only observe the two quasar components; the complex structure of the HST PSF is well seen. From the F814W observations, we detect the lensing galaxy G near the brightest component A. The lower panels correspond to the results of PLUCY deconvolutions using appropriate simulated TinyTim PSFs. An inset (zoomed by a factor 2) illustrates the deconvolved image of the galaxy with low cuts in the lookup table.

A set of approximately 100 simulated PSFs was computed by means of the TinyTim program (Krist 1997) for different values of the focus (Zernicke parameter Z4) and of the jitter of the telescope. These numerical PSFs were then fitted to the images of HE 1104−1805 A and B with an automatic procedure described in Østensen et al. (1997). Optimal values for the Z4 and the "jitter" parameters were then derived for each individual CCD frame. Due to the breathing of the telescope, excursions of up to 7 μm were found for the focus (Z4) during the F814W observations. The optimal PSF was subsequently built with an oversampling factor of 10. An iterative procedure was used to address the problem of fitting the HST PSF peak after proper re-centering and re-binning of the final TinyTim PSF. Finally, the 2-channel PLUCY application program (Hook and Lucy 1994) was fed with those PSFs to deconvolve each single CCD frame of HE 1104−1805. The combined results of those deconvolutions are presented for the F555W and F814W filters in the lower panels of Figure 1. We also decomposed all images of HE 1104−1805 with two point-like components (their relative positions and brightnesses being the only free parameters) and one

additional exponential or gaussian profile with elliptical isophotes. After subtraction of the optimal model, we only observe insignificant residuals around the point-like components.

We have then followed the standard HST photometric procedure of integrating the flux of point sources in the classical $0\farcs5$ aperture (Whitmore 1997) and rely upon the values of the PHOTFLAM keyword appearing in the header of the PC1 frames. We derived the individual magnitudes of HE 1104−1805 A, B in the Johnson V and Kron-Cousins I_c systems (see Table 1) from the F555W and F814W in-flight magnitudes taking color corrections into account (Holtzman et al. 1995). The magnitude for the galaxy is derived in two steps. First we fit the images with two numerical PSFs and an exponential model for the galaxy. The measurements for the galaxy then result from the integration of the flux, remaining after the removal of the two fitted quasar components, using two apertures with radii $0\farcs95$ and $1\farcs35$.

Object	A	B	G($0\farcs95$)	G($1\farcs35$)	B−A
V	16.74	18.48	>23	>23	1.74
I_c	16.33	17.93	20.93	20.88	1.60
θ	$0\farcs0$	$3\farcs193$	$1\farcs03$	$1\farcs03$	$3\farcs193$

Table 1. Photometry and relative angular separation (θ) of the A & B components of HE 1104−1805 and of the lensing galaxy G. The photometric calibration is accurate to ±0.05 mag. Radii of the aperture used to evaluate the magnitudes of the galaxy are given in parentheses. The error bars for the galaxy magnitude are estimated to be 0.1 mag.

3. PC1 Direct Imaging of J03.13

Following the ground-based identification of two resolved point-like images for the quasar J03.13 (see Claeskens et al. 1996), we proposed to image this interesting system with the WFPC2 planetary camera (PC1) through two wideband filters in order to search for possible structure of the QSO images at $\simeq 0\farcs1$ angular scales and also to possibly set additional constraints on the lensing model. Based on the photometry reported for this system by Claeskens et al. (1996), we chose the ADC channel with 14 e^-/ADU gain and integration times of 160 (resp. 400 and once 300) seconds, to avoid the saturation of the brightest QSO image through the F555W (resp. F814W) broadband filters. Given the two orbits allocated to this HST direct imagery program (ID 5958), our strategy has been to obtain 5 (resp. 6) such PC1 exposures with the F555W (resp. F814W) filters on November 28, 1995. Each of these exposures has been offset by $\simeq 1\farcs6$ in order to optimally dither the QSO images and possibly detect faint structures at small angular scales.

Composite F555W and F814W images of J03.13 made after proper recentering and coaddition of the single PC1 frames are shown on the left panels of Figure 2.

On these composite and on each single CCD frames, J03.13 appears to be resolved as two point-like components. No trace of a third compact image or of a faint intervening galaxy is visible. The somewhat extended core and knotty-like structures seen for each single image component are essentially due to the complex shape of the combined "HST + WFPC2 + filters" point spread function (PSF). These images have been analysed using the same procedure as for the case of HE 1104−1805 discussed above.

Combined results of the PLUCY deconvolutions are presented for the F555W (resp. F814W) filters in the upper (resp. lower) right panels of Figure 2. Given that TinyTim PSFs are not more accurate than a few tenths of a percent, the very faint residuals seen near J03.13 A and B on the deconvolved images turn out to be non significant. Using the PLUCY deconvolution algorithm, the magnitude difference between the two unresolved components is found to be 2.14 ± 0.03 and 2.16 ± 0.03 mag for the F555W and F814W filters, respectively.

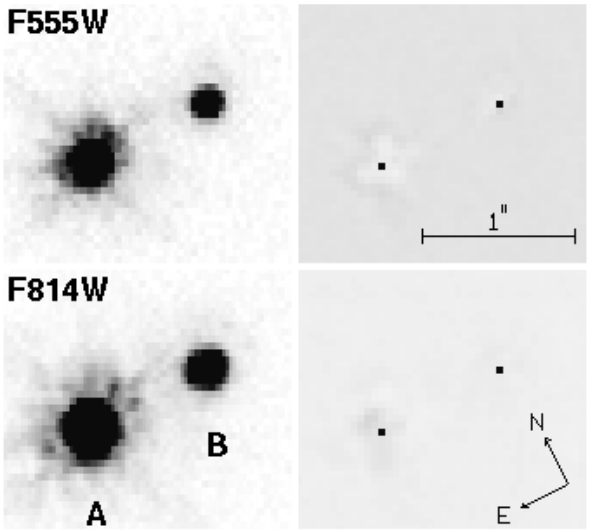

Figure 2. Composite F555W (upper left panel) and F814W (lower left panel) CCD frames of J03.13 A and B. The right panels correspond to the results of PLUCY deconvolutions using appropriate simulated TinyTim PSFs (see text). All four subimages have been normalized to the peak maximum of the A component. The faint residuals seen on the deconvolved images are well below 0.3%.

We also used the optimal TinyTim PSFs selected above and the automatic photometric fitting technique described in Østensen et al. (1997) to decompose all images of J03.13 with two point-like components, their relative positions and brightnesses being the only free parameters. After subtraction of the best fitted double PSFs, no significant residuals are seen. The angular separation between the two components is found to be $0\farcs849 \pm 0\farcs001$ and the magnitude difference $\Delta\,\mathrm{m} = 2.14 \pm 0.03$ mag for both I and V.

We have derived the integrated magnitudes of J03.13 to be $V = 17.3$ and $I = 16.8$ mag, each $\pm$ 0.1.

4. FOS Observations of J03.13

To definitely prove the spectral similarity between the J03.13 A and B images ("to be or not to be lensed"), we have taken on October 28, 1996 FOS spectra at the positions of these two components, and at a third position C, symmetric from B with respect to A. These FOS/RD spectra were obtained with the grating G650L (central wavelength of 4400 Å, FWHM $\simeq$ 30.5 Å, COSTAR deployed) and the small 0.5 (actually $0\farcs43$) circular aperture. The spectra of J03.13 A and B are shown in Figure 3.

We find that, apart from a multiplicative constant of 7.5 $\pm$ 0.7 (corresponding to a magnitude difference Δm = 2.2 $\pm$ 0.1), the spectra of J03.13 A and B are identical. We have also reproduced in Figure 3 the residual spectrum $A - B \times 7.5$ showing that, apart from a few datapoints near the emission line peaks—which are undersampled by the FOS—and the MgII absorption lines at $z = 1.085$, the spectra of J03.13 A and B do indeed look quite similar. Spectrum of C probes for the possible contamination of component B by A, which turns out to be absolutely negligible. We confirm the emission-line redshift $z_{\mathrm{em}} = 2.545$ reported by Claeskens et al. (1996) as well as the two absorption line systems at $z_{\mathrm{abs}} = 2.344$ and $z_{\mathrm{abs}} = 1.085$ (the latter one being only detected from its MgII resonance lines in the spectrum of image A).

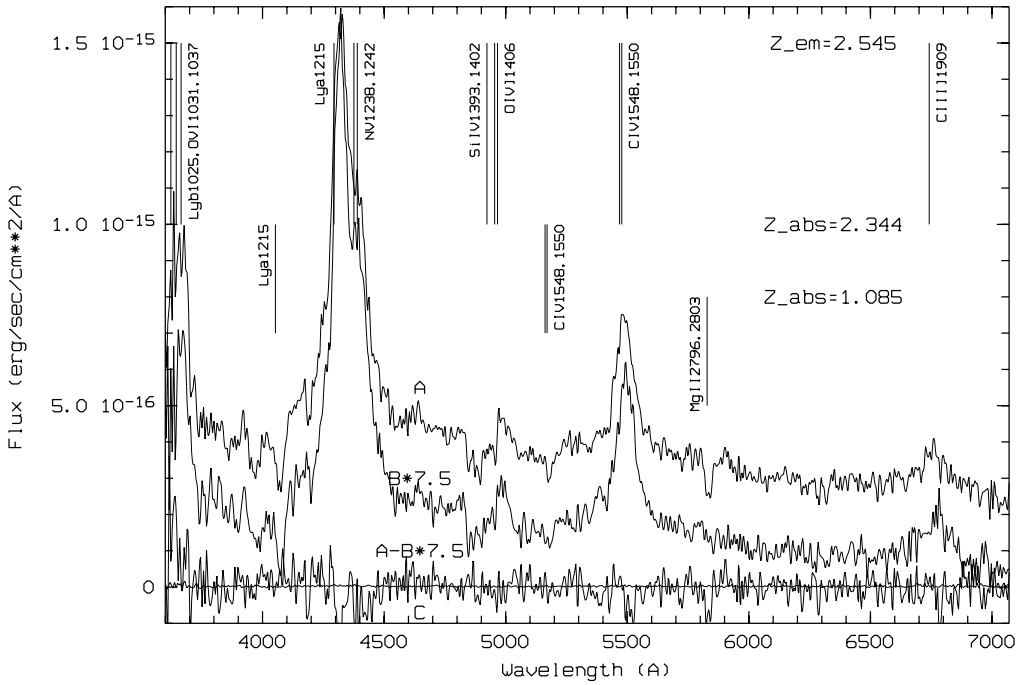

Figure 3. FOS spectra of (A) J03.13 A, (B) J03.13 B after multiplication of its flux by 7.5 and a vertical offset by -2.010^{-16} erg/sec/cm^2/Å, (C) a fiducial target at the symmetric position of B with respect to A for probing light contamination from the latter component and (D) the residual spectrum of $A - B \times 7.5$. The QSO emission and two intervening absorption line systems are identified with vertical lines and labels at different redshifts (see text).

5. Conclusions

5.1. The Gravitational Lens of HE 1104−1805 A and B

The detection of a very red galaxy located between the two components of HE 1104−1805 proves the validity of the gravitational lensing hypothesis to explain this interesting object. The claim that a microlensing event is occuring for image A, proposed to explain the color differences between A and B (Wisotzki et al. 1993, 1995), is fully consistent with a more detailed analysis reported elsewhere (Remy et al. 1997b).

Combining the present HST data with ground-based IR and optical observations (Remy et al. 1997b), the lens is most likely found to be an elliptical galaxy with redshift $0.95 < z < 1.4$. This leads to a coherent scenario in which one can also explain the two main absorption line systems observed in the spectra of the quasar components. The $z = 1.32$ absorption is produced in the spectra of A and B by the deflector (a bright elliptical with $\mathcal{L} \approx 4.6\mathcal{L}^*$). Nevertheless, a smaller value for the redshift of the lens cannot be excluded. The hypothesis of a lensing galaxy at $z = 1.66$ is poorly supported by the present observations. The $z = 1.66$ absorption system is probably produced by absorbing gas in an yet unrevealed disk galaxy.

A singular isothermal sphere lens model with an additional shear term can easily explain the observed flux ratio between A and B (Remy et al. 1997b). The galaxy is found to be very massive. Its mass-to-light ratio does not much depend on redshift. For a deflector at $z = 1.32$, this ratio is estimated to be $\mathcal{M}/\mathcal{L} \sim 11\, h_{50}\, \mathcal{M}_\odot/\mathcal{L}_\odot$, a typical value for an elliptical lensing galaxy. An excess of dark matter is not required to account for this system.

The physical origin of the additional shear is unknown. It may originate in an asymmetry of the galaxy gravitational potential or in the combined effect of several foreground galaxies located near the projected position of the quasar.

5.2. The Gravitational Lens System J03.13

Direct imagery of J03.13 with the PC1 camera clearly reveals that this bright and distant quasar consists of two point-like components having an angular separation of $0\farcs849 \pm 0\farcs001$ and a magnitude difference $\Delta\,\mathrm{m} = 2.14 \pm 0.03$ mag in V and I.

Low resolution FOS spectra of J03.13 A and B show that these two components are lensed images of a same quasar at redshift $z_{\mathrm{em}} = 2.545$, with a common absorption line system at $z_{\mathrm{abs}} = 2.344$; the MgII absorption resonance lines at $z_{\mathrm{abs}} = 1.085$ are only detected in the spectrum of the A component.

Acknowledgments

This paper is based on observations made with the NASA/ESA Hubble Space Telescope, obtained at the Space Telescope Science Institute, which is operated by the Association of Universities for Research in Astronomy, Inc., under NASA contract NAS 5-26555. Part of this work has been supported by the SSTC/PRODEX (HST observations of gravitational lenses) project and a belgian FNRS grant (travel support for JS).

References

Claeskens J.-F., Surdej, J., & Remy, M., 1996, A&A, 305, L9

Grundahl, F., Hjorth, J., & Sørensen, A.N., 1995, Highlights of Astronomy, 10, 658

Holtzman, J. A., et al., 1995, PASP, 107, 1065

Hook, R. A., & Lucy, L. B., 1994, in *The restoration of HST images and spectra—II*, R. Hanisch & R. White (eds.), p. 86

Krist, J., 1997, *WFPC2 ghosts, scatter and PSF field dependence*, postcript document available via the STScI WWW page

Østensen, R., Remy, M., Lindblad, P. O., Refsdal, S., Stabell, R., et al., 1997, A&AS, in press

Remy, M., Surdej, J., Baggett, S., & Wiggs, M., 1997a, this volume

Remy, M., Claeskens, J.-F., Surdej, J., Hjorth, J., Refsdal, S., Wucknitz, O., Sørensen, A. N., & Grundahl, F., 1997b, New Astronomy, submitted

Remy, M., Claeskens, J.-F., & Surdej, J., 1998, in preparation

Smette, A., Robertson, J. G., Shaver, P. A., Reimers, D., Wisotzki, L., & Köhler, T., 1995, A&A, 113, 199

Surdej, J., Claeskens, J.-F., Crampton, D., Filippenko, A. V., Hutsemékers, D., et al., 1993, AJ, 105, 2064

Surdej J., Claeskens J.-F., Remy, M., Refsdal, S., Pirenne, B., Prieto, B., & Vanderriest, Ch., 1997, A&A, in press

Whitmore, B., 1997, *Photometry with the WFPC2*, postcript document available via the STScI WWW page

Wisotzki, L., Köhler, T., Kayser, R., & Reimers, D., 1993, A&A, 278, L15

Wisotzki, L., Köhler, T., Ikonoumou, M., & Reimers, D., 1995, A&A, 297, L59